Retrieval of stratospheric NO_3 vertical profiles from SCIAMACHY lunar occultation measurement over the Antarctic

L. K. Amekudzi, B.-M. Sinnhuber, N. V. Sheode, J. Meyer, A. Rozanov, L. N. Lamsal, H. Bovensmann, and J. P. Burrows

Institute of Environmental Physics and Remote Sensing, University of Bremen, Bremen, Germany

[1] NO_3 vertical profiles have been retrieved over the Antarctic ($60°-90°$S) from the Scanning Imaging Absorption Spectrometer for Atmospheric Cartography (SCIAMACHY) lunar occultation spectra, using the visible spectral band (610–680 nm) containing NO_3 absorption bands at 623 and 662 nm. The retrieved NO_3 profiles agree well with calculations from a photochemical model constrained by retrieved O_3 and analyzed temperatures in the altitude range between 24 and 45 km. Below about 35–40 km, observed NO_3 is well reproduced by photochemical steady state calculations. Differences between observed and modeled NO_3 are within the estimated accuracy of 20–35%, demonstrating the consistency of the NO_3 retrieval and model.

Citation: Amekudzi, L. K., B.-M. Sinnhuber, N. V. Sheode, J. Meyer, A. Rozanov, L. N. Lamsal, H. Bovensmann, and J. P. Burrows (2005), Retrieval of stratospheric NO_3 vertical profiles from SCIAMACHY lunar occultation measurement over the Antarctic, *J. Geophys. Res.*, *110*, D20304, doi:10.1029/2004JD005748.

1. Introduction

[2] The presence of nitrate radical, NO_3, in the stratosphere, influences significantly the chemistry in this region of the Earth's atmosphere. At night, NO_3 controls the concentration of odd nitrogen, NO_x ($NO + NO_2$) in both the troposphere and the stratosphere. NO_3 plays an active role as a radical intermediate molecule in the conversion of NO_x to NO_y ($N_2O_5 + HNO_3$) which affects the abundance and diurnal variability of NO_2, a molecule which contributes significantly to stratospheric ozone chemistry.

[3] In the absence of heterogeneous processes the stratospheric nighttime NO_3 chemistry is believed to be governed by a relatively simple scheme involving NO_2, O_3, and N_2O_5 molecules:

$$NO_2 + O_3 \longrightarrow NO_3 + O_2, \qquad (1)$$

$$NO_3 + NO_2 + M \longrightarrow N_2O_5 + M, \qquad (2)$$

$$N_2O_5 + M \longrightarrow NO_3 + NO_2 + M. \qquad (3)$$

Reaction (1) is the main formation process of NO_3 and the nitrate radical is removed from the atmosphere by reacting with NO_2 to form N_2O_5 (reaction (2)), a reaction whose rate constant is temperature-dependent [*Norton and Noxon*, 1986; *Sanders et al.*, 1987; *Wangberg et al.*, 1997]. The reverse reaction (3) serves as an additional NO_3 formation

source when N_2O_5 in reaction (2) is thermally decomposed to form NO_2 and NO_3. Assuming a steady state based on reaction (1) to reaction (3), the concentration of NO_3 can be calculated as

$$[NO_3] = \frac{k_1[O_3]}{k_2[M]} + \frac{k_3[N_2O_5]}{k_2[NO_2]}, \qquad (4)$$

where k_1, k_2, and k_3 are the reaction rate constants of reactions (1), (2), and (3), respectively, and M is the number density of air. For relatively low stratospheric temperatures the reaction (3) is slow, and the second term in the right-hand side of equation (4) can be neglected. For the this conditions, NO_3 concentration is approximated as [*Norton and Noxon*, 1986; *Sanders et al.*, 1987]

$$[NO_3] = \frac{k_1\,[O_3]}{k_2\,[M]}, \qquad (5)$$

the lifetime of NO_3, τ, being

$$\tau = \frac{1}{k_2\,[NO_2]\,[M]}. \qquad (6)$$

During the polar winter and spring, N_2O_5 reacts on the surface of stratospheric sulphate aerosol (SSA) heterogeneously to form HNO_3 and polar stratospheric clouds (PSC).

[4] The first atmospheric measurements of NO_3 were reported by *Noxon et al.* [1978], who used a ground-based scanning spectrometer to measure NO_3 abundance above Fritz Peak observatory at latitude $40°$N using the moonlight.

Other ground-based NO$_3$ measurements using the Moon as light source were reported [*Platt et al.*, 1981; *Gelinas and Vajk*, 1981; *Norton and Noxon*, 1986; *Solomon et al.*, 1989b; *Smith and Solomon*, 1990]; these measurements show geographical, altitudinal, strong diurnal and seasonal variations in NO$_3$ concentration. The first ground-based NO$_3$ measurements over Antarctica were reported by *Sanders et al.* [1987]. These measurements were carried out at McMurdo station, Antarctica (77.8°S) and other measurements at McMurdo station during the fall, winter, and spring seasons were reported [*Solomon et al.*, 1989b, 1993]. NO$_3$ vertical profiles have been derived from balloon-borne stellar occultation measurements at midlatitudes [*Naudet et al.*, 1981, 1989; *Rigaud et al.*, 1983]. According to *Naudet et al.* [1989], nighttime stratospheric mixing ratios of NO$_3$ are between 5 and 160 ppt in the altitude range of 22–38 km. NO$_3$ vertical profiles have also been inferred from balloon-borne instrument using the Moon as light source [*Renard et al.*, 1996, 2001]. The ground-based and balloon-borne platforms however have not provided broader geographical coverage of the nitrate radical. Recently satellites have been used for the first time for lunar occultation measurements of nighttime atmospheric trace gases; these instruments are Scanning Imaging Absorption Spectrometer for Atmospheric Cartography (SCIAMACHY) [*Burrows et al.*, 1988; *Bovensmann et al.*, 1999] and Stratospheric Aerosol and Gas Experiment (SAGE III) [*McCormick et al.*, 2002].

[5] Scanning Imaging Absorption Spectrometer for Atmospheric Cartography (SCIAMACHY) is a passive remote sensing moderate-resolution imaging, UV-Vis-NIR spectrometer on board the European Space Agency's (ESA) Environmental Satellite (Envisat) launched in March 2002 from Kourou, French Guiana. The instrument was developed to contribute to a better understanding of ozone chemistry as well as pollution and climate monitoring issues. SCIAMACHY has eight channels, covering the spectral range of 240–2380 nm, with a spectral resolution of 0.24–1.48 nm [*Bovensmann et al.*, 1999]. SCIAMACHY is one of the first space-borne instruments to measure NO$_3$. NO$_3$ is also measured by Ozone Monitoring by Occultation of Stars (GOMOS), on board Envisat, using stellar occultation technique [*Marchand et al.*, 2004].

[6] The goal of this study is to present the first vertical profiles of NO$_3$ retrieved from SCIAMACHY lunar occultation measurements over the Antarctic continent. A brief description of lunar occultation measurements is presented in section 2. Section 3 describes the retrieval technique and results. A comparison of retrieved NO$_3$ with model calculations is presented in section 4. Section 5 summarizes the results.

2. Measurements and Data

2.1. Lunar Occultation Measurement

[7] The SCIAMACHY instrument performs lunar occultation measurements in the southern hemisphere of the Earth's atmosphere, between 30° and 90° latitude, during local nighttime. SCIAMACHY Moon visibility is possible above the northern hemisphere however, these events usually coincide with sunrise. While sunrise is mainly defined by the relatively stable position of the Sun with respect to Envisat's orbital plane, the properties of moonrise in SCIAMACHY's limb field of view (LFOV) are determined by the orientation of the lunar orbital plane with respect to Envisat's orbital plane and the ecliptic. In this plane, the Moon completes one orbit within one synodic period of 29.53 days. Caused by the lunar orbital motion, the Moon moves through the LFOV from left to right at a rate of about 1° per orbit, starting lunar occultation measurement at a lunar phase of 0.6–0.7 and ending shortly after full Moon. The SCIAMACHY measurements are performed in Moon pointing (staring) mode similar to Halogen Occultation Experiment (HALOE) [*Russell et al.*, 1993].

[8] The SCIAMACHY instrument's Instantaneous Field Of View (IFOV) in lunar occultation mode is 0.045° in vertical direction and 1.8° in horizontal direction, the latter being larger than the apparent diameter of the Moon, which is approximately 0.5°. To effectively track the Moon, the Moon Follower (MF) device is adjusted to the brightest point of the apparent Moon, as the Moon rises above the Earth's horizon. Starting at approximately 17 km, the MF follows the Moon up to 100 km [*Noël et al.*, 2000]. Below this critical altitude (17 km), apparent angular rate of the rising true Moon is significantly higher than that of the rising refracted images, as a result, tracking the rising Moon becomes almost impossible for the MF device. Above 100 km, Moon measurements are performed for instrument calibration purposes. The integration time for SCIAMACHY lunar occultation measurement is 1.0 s with a vertical resolution of ∼3 km and horizontal resolution in the range of 30–40 km.

[9] SCIAMACHY lunar occultation can be successfully executed only when the lunar visibility occurs on the nightside. Because of the large field of view (2.1° × 2.1°), the MF device always detects in dayside occultations a strong signal (stray light) from the bright Earth's atmosphere at lower lunar altitudes in addition to the moonlight, which prevents the MF device from acquiring and tracking the Moon. In addition, variability in the lunar albedo, the perturbation effect of the motion of the Moon, and seasons are other challenges faced by interpretation of SCIAMACHY lunar occultation data [*European Space Agency*, 1994]. The useful SCIAMACHY lunar occultation events where the Moon rises on the nightside are on the average 6 days per month and 3 to 6 months in the year. Lunar occultation measurements performed in 2003 are located in the latitude band of 60°–90°S (see Figure 1). These measurements were carried out from February to June 2003 and time of these measurements correspond to solar zenith angles (SZA) between 95° and 115°.

2.2. Data Source

[10] The data used for the retrieval were extracted from the SCIAMACHY lunar occultation uncalibrated (level 0) data. The extraction involves removal of dead pixels, dark current correction and wavelength calibration. This is followed by the extraction of lunar spectrum $I^m(h_i, \lambda)$ at each tangent height h_i and spectral point λ between 17 and 100 km (measured lunar radiance), where i is the tangent height index. In addition, the lunar reference spectrum $I_o(\lambda)$ is extracted from the measurement above 100 km (measurement at 120 km). The transmission
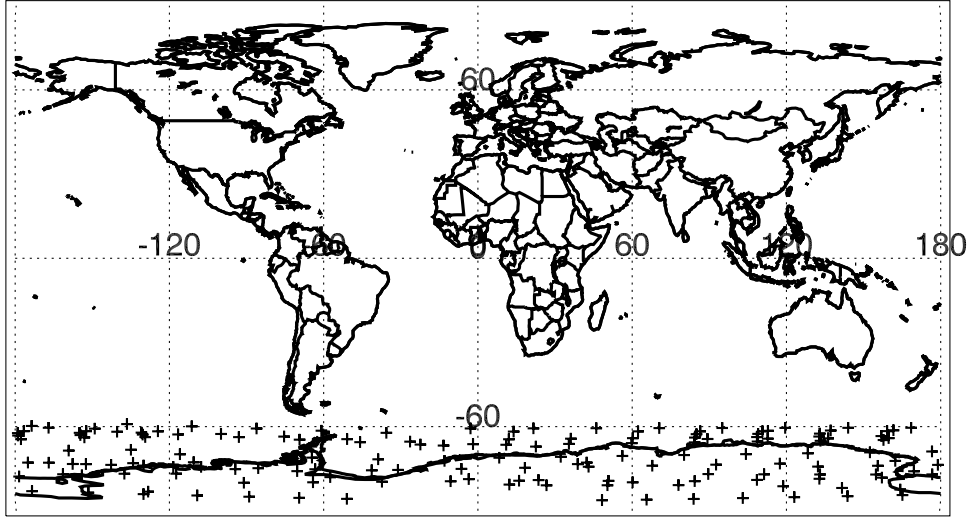
Figure 1. SCIAMACHY lunar occultation geographical coverage for 2003. Crosses indicate the location of measurements.

spectra $\Upsilon^m(h_i, \lambda)$ containing atmospheric spectral lines are obtained by dividing the measured lunar radiance at each tangent height by the lunar reference spectrum above the atmosphere.

3. Retrieval Technique and Result

[11] In this section, a brief discussion of the forward model, the inversion scheme, and the retrieval outputs are presented.

3.1. Forward Model

[12] The primary aim of a forward model in the retrieval of atmospheric parameters is to include the essential physics of measurements and all obtainable characteristics of the instrument to enable a realistic simulation of real measurement from the instrument to be modeled. For evaluation of SCIAMACHY occultation measurements, a fast and accurate radiative transfer model (RTM) was developed at the Institute of Environmental Physics/Remote Sensing, University of Bremen [*Rozanov*, 2001]. Given the appropriate observing conditions (viewing angle), a priori profile, absorption cross section of trace gases, atmospheric temperature and pressure distributions, and a suitable instrument slit function, the RTM simulates the lunar transmitted radiance measured by the SCIAMACHY instrument and also computes the Jacobian matrix of the derivatives of these simulated measurements with respect to the retrieval parameters. The simulated atmospheric transmission spectra are generated by the occultation RTM at a set of tangent heights appropriate to the lunar occultation measurement sequence. The simulated transmission $\Upsilon^s(h_i, \lambda)$ for a given tangent height, h_i, and wavelength, λ, is given by

$$\Upsilon^s(h_i, \lambda) = \int_\Omega \int_{\Delta\lambda} S(\lambda, \lambda')F(\omega)e^{-\tau(h_i, \lambda')}d\lambda'd\omega, \quad (7)$$

where $\Delta\lambda$ is the total width of SCIAMACHY slit function $S(\lambda, \lambda')$, Ω is the field of view of the instrument, and $F(\omega)$ is the apparatus function. $\tau(h_i, \lambda')$ is the full optical depth

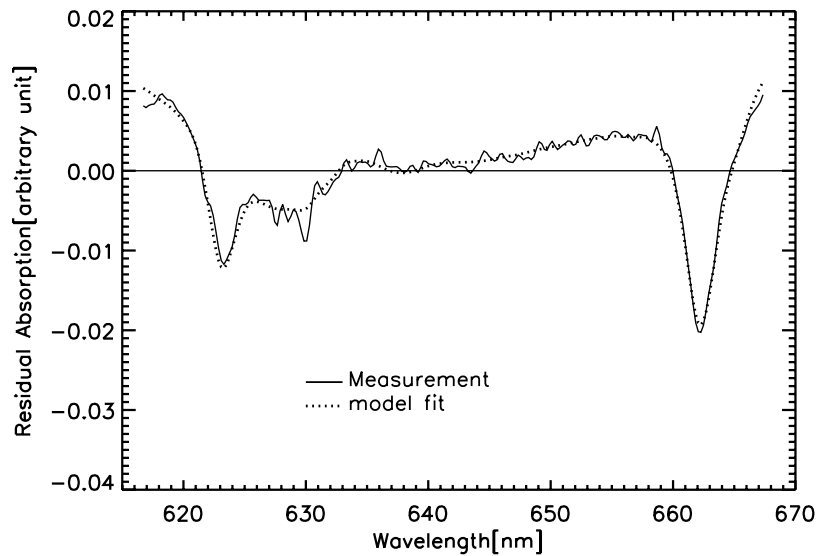along the line of sight through the atmosphere. The resulting Jacobian matrix is given as

$$W^j(h_i, \lambda) = \frac{\delta\Upsilon(h_i, \lambda)}{\delta x_j}x_j, \quad (8)$$

where $W^j(h_i, \lambda)$ is the weighting function, x_j is the concentration of the trace gas of interest at a certain altitude level, i denotes the tangent height index, and j denotes the retrieval parameter index (trace gas concentrations at a particular height level).

[13] NO$_3$, O$_3$, and O$_2$ were fitted together using the spectral window of 610–680 nm within the Chappius band of ozone, allowing the intense NO$_3$ (0-0) absorption bands at 623 and 662 nm to be used. Within the chosen spectral window it is important to properly correct for water vapor interference [*Solomon et al.*, 1989a]. This was achieved by incorporating a line-by-line spectral simulation code in the forward model to fit and thereby remove water vapor contribution [*Rothman et al.*, 1998]. Similarly, the line-by-line simulation code was used to calculate the absolute cross sections of O$_2$ needed for modeling of the transmission spectra.

[14] In order to remove broadband absorption features of the atmosphere and instrument from the measured spectrum, a third-order polynomial is subtracted at each tangent height. This is done for the logarithms of measured and reference lunar occultation radiance, the logarithm of simulated transmission spectra and the logarithmic weighting functions to obtain resulting differential spectra $\tilde{I}^m_i(\lambda)$, $\tilde{I}_o(\lambda)$, $\tilde{\Upsilon}^s_i(\lambda)$, and $\tilde{W}^j_i(\lambda)$. Shift and squeeze correction is performed to reduce errors resulting from wavelength calibration and doppler shift by minimizing the following quadratic form:

$$\|\tilde{\Upsilon}^s_i(\lambda) + \sum_j \tilde{W}^j_i(\lambda)\frac{\Delta x^j}{x^j} - \tilde{I}^m_i(\lambda)$$
$$+ \tilde{I}_o(\lambda) - \left(b^s_{shi} - b^s_{sq}\lambda\right)\frac{\delta\tilde{\Upsilon}^s_i(\lambda)}{\delta\lambda}$$
$$- \left(b^m_{shi} - b^m_{sq}\lambda\right)\frac{\delta\tilde{I}_o(\lambda)}{\delta\lambda}\|^2 \longrightarrow \min. \quad (9)$$

Figure 2. Absorption residual at 39 km tangent height (for the 12 March 2003 orbit 5390 and SZA 105.8). The dotted line represents the differential weighting functions of NO$_3$, and the solid line is the measured differential absorption spectrum of NO$_3$.

$\tilde{W}_i^j(\lambda)$ is the vertically integrated weighting function and $\Delta x^j/x^j$ represents a scaling of the vertical profiles. The last two terms in equation (6) account for the shift and squeeze correction within the retrieval code. The shift and squeeze correction is applied for the ratio of the modeled transmission spectra with respect to the measured transmission spectra. These are represented by the coefficients b_{shi}^s and b_{sq}^s. The shift and squeeze correction is also applied for occultation measurements at the reference tangent altitude with respect to the measurements at atmospheric tangent altitude, represented by the coefficients b_{shi}^m and b_{sq}^m.

[15] Figure 2 shows example of the spectral fit at 39 km tangent height for 12 March 2003, corresponding to Envisat orbit number 5390, and solar zenith angle (SZA) of 105.8. The dotted line is the differential weighting function of NO$_3$ and the solid line represents the measured differential absorption spectrum of NO$_3$.

3.2. A Priori Data Source

[16] The geometric height is used as vertical coordinate for both the RTM and the inversion scheme. The atmosphere is divided into 100 equidistant layers between 0 and 100 km altitude. The NO$_3$ absorption cross section at 298 K was taken from Jet Propulsion Laboratory (JPL) [*Sander et al.*, 1997] and O$_3$ absorption cross sections at five different temperatures were measured at University of Bremen [*Burrows et al.*, 1998]. Temperature, pressure, O$_2$ and O$_3$ a priori profiles were taken from the U.S. Standard Atmosphere [*NASA*, 1976]. The a priori profile of NO$_3$ was taken from the results [*Schlieter*, 2001], which is based on ground-based lunar occultation measurements [*Aliwell*, 1995]. Tangent height information was derived from an independent fitting and subsequent retrieval of O$_2$ profiles [*Meyer et al.*, 2004].

3.3. Inversion Scheme

[17] The final step of the retrieval is to derive vertical profile information from measurement using the optimal

estimation (OE) method [*Rodgers*, 1976]. At this step, the following linear equation has to be solved

$$y = K(x - x_o) + \epsilon, \tag{10}$$

where y is the measurement vector containing the differences between the simulated and measured differential lunar transmission spectra at all available spectral points in the selected spectral range and all selected tangent heights. x is the state vector containing trace gas concentrations in a specified altitude range for all species to be retrieved from the atmosphere and x_o is the a priori state vector. K is linearized forward model operator containing the differential weighting functions and ϵ expresses all possible errors.

[18] The retrieval solution is obtained iteratively following the Newton iteration scheme, where the profile result x_i is used as linearization point for the $(i + 1)$th iteration. The optimal estimation solution for x_{i+1} is given by

$$x_{i+1} = x_o + \left(K_i^T S_y^{-1} K_i + S_a^{-1}\right)^{-1} K_i^T S_y^{-1} (y - y_i + K_i(x_i - x_o)), \tag{11}$$

where S_a is the a priori covariance matrix and S_y the measurement error covariance matrix. The superscripts T and -1 represent matrix transpose and inverse, respectively. The corresponding solution covariance matrix $\hat{S}$ is given as

$$\hat{S} = \left(\hat{K}^T S_y^{-1} \hat{K} + S_a^{-1}\right)^{-1}. \tag{12}$$

3.4. Averaging Kernel and Precision

[19] The vertical resolution and the sensitivity of each retrieval can be characterized by the averaging kernels, which couple the true profile and the retrieved profile of a
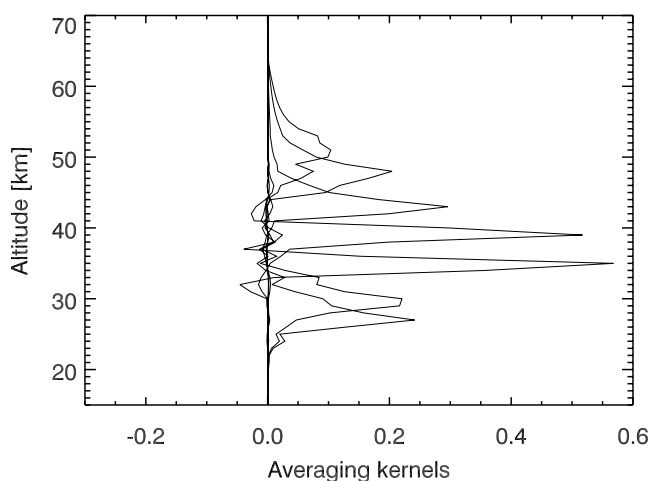
Figure 3. Averaging kernels of selected altitudes for the retrieved profile of NO_3. This result is based on the vertical resolution of the retrieval (1 km height grid).

particular trace gas. The averaging kernel matrix, A, is given as

$$A = \frac{\partial \hat{x}}{\partial x}, \qquad (13)$$

where $\hat{x}$ is the retrieved atmospheric state vector and x is the true atmospheric state vector. Averaging kernels for selected altitudes for retrieved NO_3 are shown in Figure 3. From the averaging kernel, the highest sensitivity of NO_3 is at 35 km followed by the sensitivity at 40 km. The sensitivity at 27–30 and 45 km are approximately half of the sensitivity at 35 km. Below 20 and above 60 km, no significant information about the NO_3 concentration is observed.

[20] Precision of the retrieved NO_3 profile was calculated using a priori covariance of 90% and signal-noise ratio of 1000. In the absence of systematic error, NO_3 vertical profile distribution can be retrieved from SCIAMACHY lunar occultation data with an accuracy better than 20% and the retrieval error is less than 10% for regions of higher sensitivity (35–45 km) (see Figure 4).

3.5. Number Density Distributions

[21] The retrieved NO_3 is presented in Figure 5. Figure 5 shows the zonal mean profiles of NO_3 concentration retrieved from SCIAMACHY lunar occultation measurement between March and June 2003. The highest concentration of retrieved NO_3 were in the moderately high latitude (60–65°S), corresponding to altitude range of 36–40 km. These high values were mainly due to the contribution from measurement data of March where the stratosphere was relatively warm. The low values of retrieved NO_3 were observed in the high latitude (70–85°S). These values were the contribution from April, May, and June where the temperature in the stratosphere was relatively low.

3.6. Measurement and Retrieval Errors

[22] In addition to the statistical error of less than 20% (see Figure 3b), other possible significant errors that could be introduced into the results are discussed in this section.

[23] The uncertainty in the NO_3 absolute cross sections is at least 4% [Orphal et al., 2003]. The water vapor absorp-

tion band (640–665 nm) overlaps with NO_3 absorption line at 662 nm although this effect was considered in the forward model part of the retrieval code, it could introduce a systematic error in the simulated transmission spectra, the Jacobian and hence the retrieved profiles. Because of varying brightness of the Moon, higher detector noise and stray light could influence the measured lunar signal and could introduce a random error of less than 5% in the measurement. This effect was seen in some of the residual transmission spectra. Although shift and squeeze correction has been used in the retrieval code to correct for wavelength shift, a wavelength calibration error of approximately 1% could remain in the retrieval result. Although retrieval of O_2 is used to improve the information on tangent height, there could still be an error of less than 1 km resulting from a pointing error of less than 0.012°, which could affect the number of photons absorbed [Meyer et al., 2005]. Other sources of error include systematic errors in the a priori temperature, pressure, and NO_3 profiles and smoothing error of less than 7%, as Twomey-Tikhonov regularization was applied in the retrieval process to obtain smooth NO_3 profiles. The retrieved results thus have uncertainties in the measurement and atmospheric a priori information. These uncertainties have contributed to random and systematic errors of 20–35% in the retrieved NO_3 profiles.

4. Comparison With Model Calculations

[24] In order to test, how well the SCIAMACHY measurements agree with our current understanding of the NO_3 nighttime chemistry and to check the internal consistency of the observations, the observed NO_3 profiles were compared with calculations of a photochemical model.

[25] The model is a one-dimensional (1-D) photochemical stacked box model based on the photochemical scheme from the SLIMCAT model [Chipperfield, 1999]. The model is initialized with the output of a global 2-D chemistry and transport model [Sinnhuber et al., 2003] and references therein] for the geolocation and day of the SCIAMACHY measurements. It uses reaction rate constants and photolysis cross sections according to the latest JPL recommendation
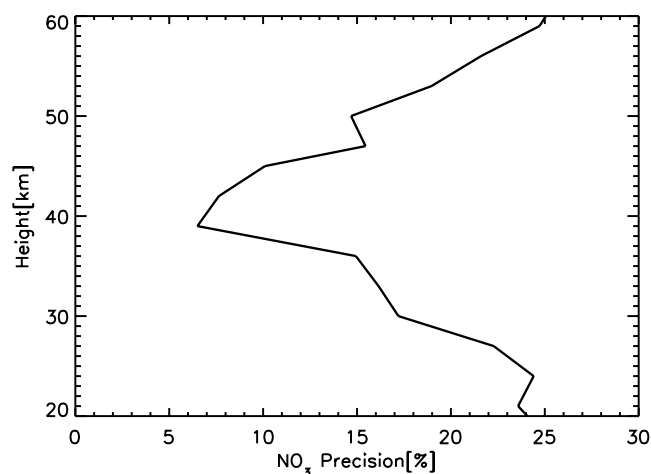
Figure 4. Precision of the retrieved NO_3 number density profile. This result is based on measurement with vertical resolution of 3–4 km.
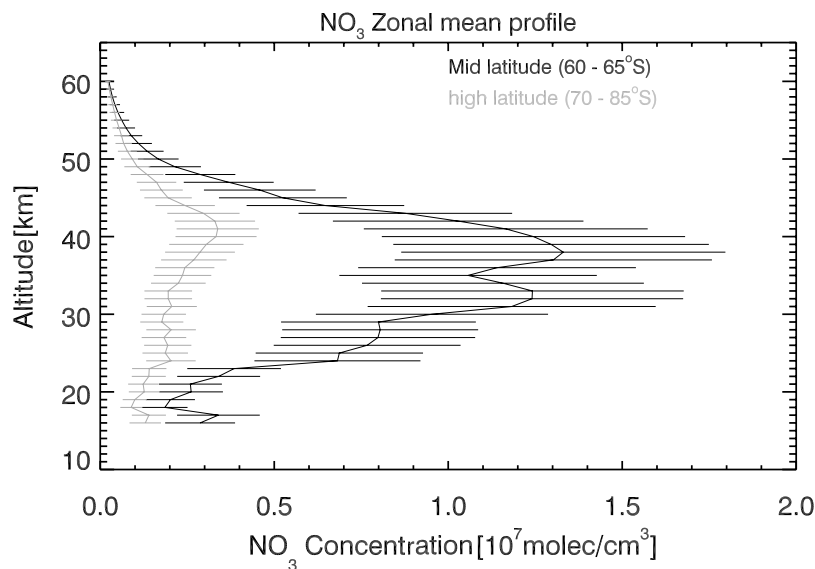
Figure 5. Zonal mean profiles of NO$_3$ retrieved from SCIAMACHY lunar occultation from March to June 2003 for latitude band of 60–65°S (black) and 70–85°S (grey). The error bars show the maximum possible error of 35%. The analysis is based on 35 profiles for 60–65°S and 95 profiles for 70–85°S.

[*Sander et al.*, 2003]. The 1-D model is constrained by temperature and pressure profiles from ECMWF analyses and ozone and NO$_2$ profiles from SCIAMACHY observations. NO$_2$ is constrained by scaling the modeled NO$_y$ (in particular NO, NO$_2$, N$_2$O$_5$, and HNO$_3$) until the modeled NO$_2$ agrees with measured NO$_2$ at the time of the SCIA-MACHY measurements.

[26] Figure 6 shows the comparison of retrieved NO$_3$ with calculated NO$_3$ from the photochemical model for 14 March 2003 (a) and for 12 April 2003 (b). In general we find a good agreement between observed and modeled NO$_3$ within the expected error of 35% between the altitude range of 24–45 km. There is a relatively large uncertainty in the modeled NO$_3$ concentration as a result of uncertainties in the temperature profile. We find that a 1 K increase in temperature increases the NO$_3$ concentration by about 6%. A 5 K uncertainty in the temperature profile, which seems realistic for the Antarctic winter stratosphere, will then result in a 30% uncertainty in the modeled NO$_3$ profile.

[27] In steady state, the nighttime NO$_3$ concentration can be described by equation (4)

$$[NO_3] = \frac{k_1[O_3]}{k_2[M]} + \frac{k_3[N_2O_5]}{k_2[NO_2]}.$$

The second term on the right-hand side of equation (4) accounts for the production of NO$_3$ due to the thermal decomposition of N$_2$O$_5$. If this term is neglected, then the nighttime steady state concentration of NO$_3$ is simple and depends only on ozone and temperature:

$$[NO_3] = \frac{k_1\,[O_3]}{k_2\,[M]}.$$

[28] In order to identify the altitude regions where the second term in equation (4) can be neglected, we assume that the concentration of N$_2$O$_5$ during night is in the same order of magnitude as the concentration of NO$_2$ or smaller.

Then equation (5) is a reasonable approximation, if the ratio k_3/k_2, which is the inverse of the equilibrium constant for reactions (2) and (3), is much smaller than the NO$_3$ concentrations. We find that for the conditions investigated here, the simple steady state formulation is expected to be valid below an altitude of about 35–40 km. This is because below 35 km the timescales of reactions (2) and (3) to reach steady state are in the order of an hour or less.

[29] Also included in Figure 6 is the steady state (SS) model calculation according to equation (5). As expected, we find a good agreement between the full time-dependent model calculations and the SS model below 35 km, where the agreement is better for the April profile where temperatures are lower. Above 40 km the SS model overestimates the NO$_3$ concentrations.

[30] A comparison between retrieved NO$_3$ profiles and profiles of NO$_3$ calculated using the SS model was carried out. The results of the monthly mean of these comparisons are shown in Figure 7; the dash lines are the retrieved NO$_3$ profiles and the solid lines with diamond points are the SS model outputs. In general the SS model outputs are in good agreement with retrieved profiles between 24 and 35 km, however some discrepancies could be observed between 30 and 35 km for March, April, and May. The SS model outputs underestimate or overestimate the NO$_3$ concentration retrieved from SCIAMACHY data between 30 and 35 km. The discrepancies are due to a large temperature gradient observed at such altitudes [*Solomon et al.*, 1993; *Renard et al.*, 2001]. Another possible source of error in the steady state profiles is the systematic error of less than 13% in the SCIAMACHY O$_3$ profiles [*Amekudzi et al.*, 2005].

5. Conclusion

[31] The first retrieved NO$_3$ profiles from SCIAMACHY lunar occultation measurements over Antarctica using Optimal Estimation (OE) method have been presented. The
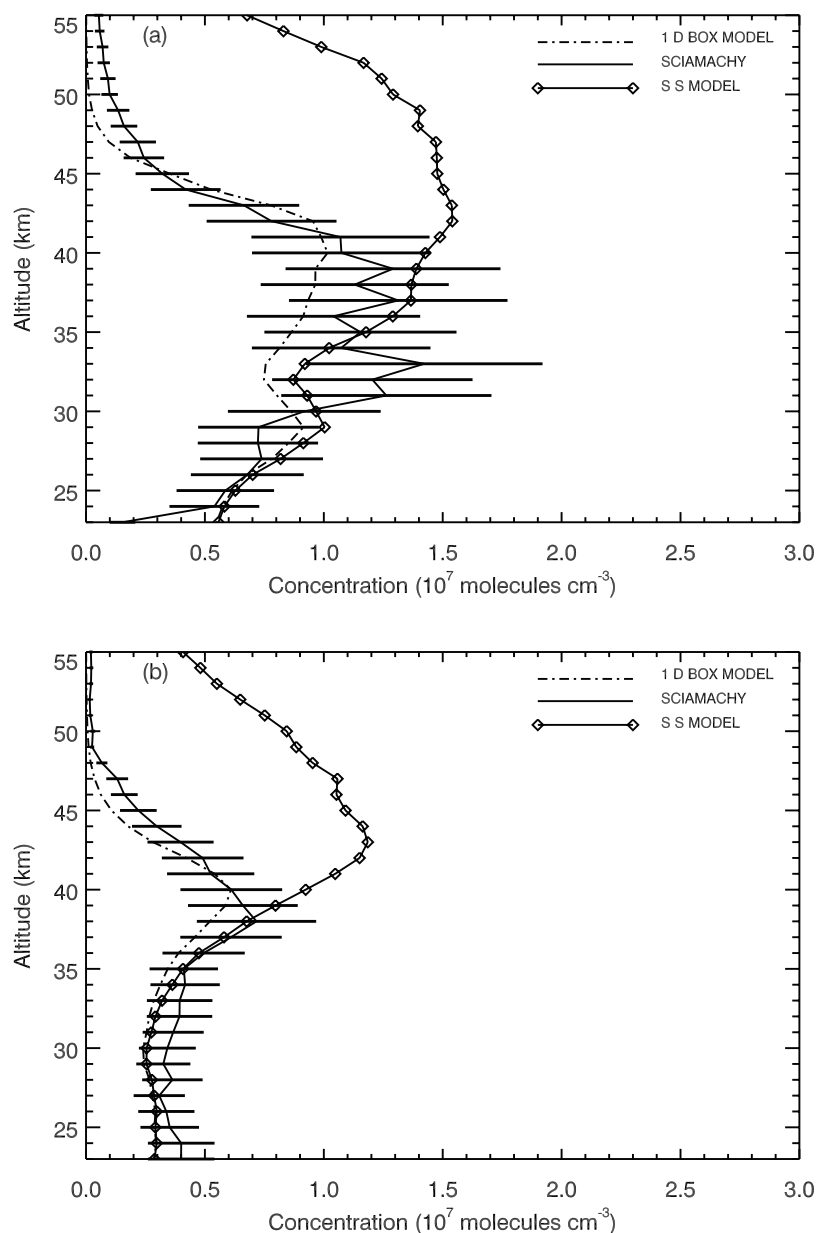
Figure 6. NO₃ profile retrieved from SCIAMACHY lunar occultation compared with NO₃ profile calculated from 1-D box model and SS model. Solid line is the retrieval result, the dash-dotted line is the 1-D box model output, and the solid line with diamond points is the SS model output. (a) Example of NO₃ profile for 14 March 2003 (at SZA 110°). (b) Example of NO₃ profile for 12 April 2003 (at SZA 115°).

spectral fits are of high quality and show absorption features of NO₃ at 623 nm and 662 nm. The retrieval error is less than 10% in the regions of higher sensitivity. The quality of the results are good, however the NO₃ profiles require further validation. A comparison of SCIAMACHY NO₃ with GOMOS NO₃ [*Marchand et al.*, 2004] is planned to be carried out in the future.

[32] The NO₃ profiles calculated from the full 1-D photochemical model are in good agreement with retrieved NO₃ profiles between 24 and 45 km within the estimated accuracy of 20–35%. SS model NO₃ agree with retrieved NO₃ in the altitude range of 24–40 km. The agreement supports the use of the steady state approximation model to calculate globally NO₃ concentrations in the middle stratosphere (24–40 km) and the use of a full photochemical model to calculate NO₃ concentration above 40 km.

[33] We observed that NO₃ chemistry in the stratosphere depends strongly on temperature and inaccuracy in stratospheric temperature of less than 5 K will contribute approximately 30% error in the observed NO₃ concentrations.

[34] A small temperature dependence of the strong (0-0) band around 662 nm of NO₃ absorption cross section due to changing population of the ground vibrational state have been observed, see *Orphal et al.* [2003, and references
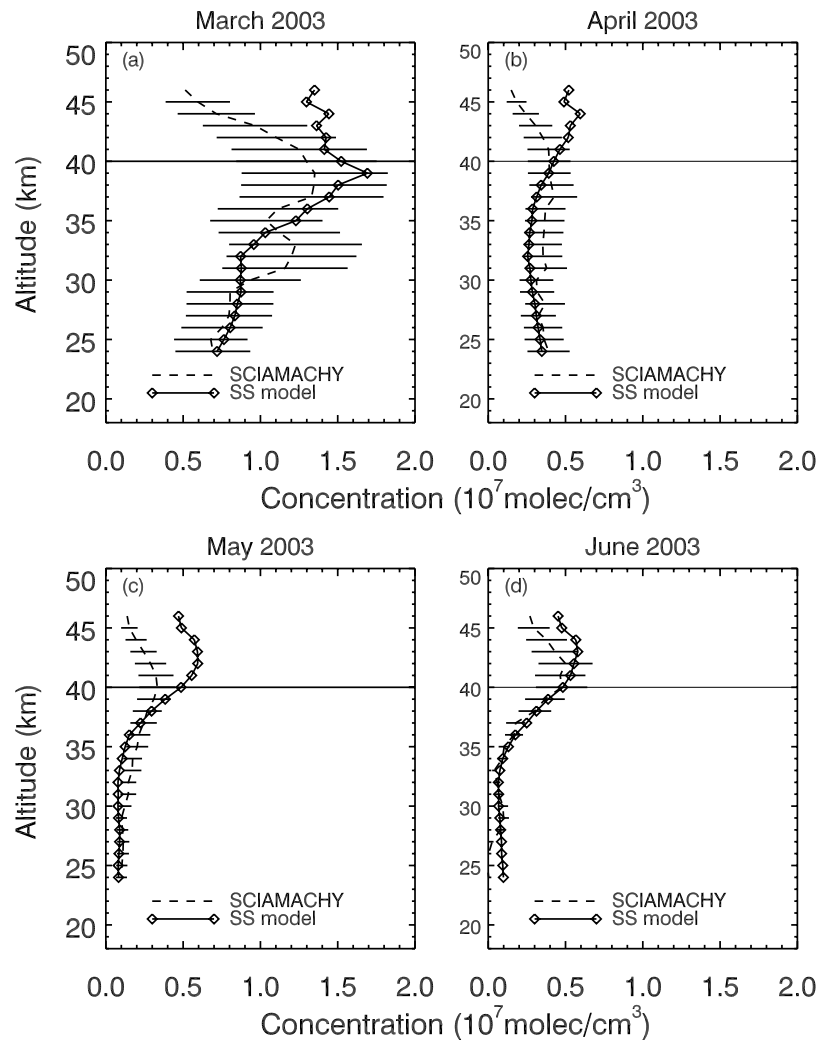
Figure 7. Monthly mean of NO₃ profile retrieved from SCIAMACHY lunar occultation compared with NO₃ profile calculated from SS model for (a) March, (b) April, (c) May, and (d) June 2003. Dashed lines are the retrieval results and solid lines with diamond points are the model outputs. The error bars show the maximum possible error of 35% as in Figure 5.

therein]. The combination of temperature and temperature-dependent cross sections will therefore improve the retrieval accuracy for NO₃.

[35] The lunar occultation measurements of SCIAMACHY demonstrate that we have a reasonable understanding of the behavior of NO₃ in the stratosphere and mesosphere. The ratio of NO₃ to N₂O₅ is very sensitive to temperature. Significant information about changing condition in the upper atmosphere will be monitored by long-term measurements of NO₃, NO₂, O₃ and temperatures from instruments like SCIAMACHY. Our understanding will benefit from linking measurements made by IR sensors such as Michelson Interferometer for Passive Atmospheric Sounding (MIPAS) and the stellar occultation measurements of GOMOS.

References

Aliwell, S. R. (1995), Measurement of atmospheric trace gases by absorption spectroscopy, Ph.D. thesis, Univ. of Cambridge, Cambridge, U.K.

Amekudzi, L. K., A. Bracher, J. Meyer, A. Rozanov, H. Bovensmann, and J. P. Burrows (2005), Lunar occultation with SCIAMACHY: First retrieval results, *Adv. Space. Res.*, *35*, doi:10.1016/j.asr.2005.03.017.

Bovensmann, H., J. P. Burrows, M. Buchwitz, J. Frerick, S. Noël, V. V. Rozanov, K. V. Chance, and A. P. H. Goede (1999), SCIAMACHY: Mission objectives and measurement modes, *J. Atmos. Sci.*, *56*(2), 127–150.

Burrows, J. P., et al. (1988), SCIAMACHY—A European proposal for atmospheric remote sensing from the ESA polar platform, report, Max-Planck-Institut für Chemie, Mainz, Germany.

Burrows, J. P., A. Dehn, B. Deters, S. Himmelmann, A. Richter, S. Voigt, and J. Orphal (1998), Atmospheric remote-sensing reference data from GOME: 1. Temperature-dependent absorption cross sections of NO₂ in the 231–794 nm range, *J. Quant. Spectrosc. Radiat. Transfer*, *60*, 1025–1031.

Chipperfield, M. P. (1999), Multiannual simulations with a three-dimensional chemical transport model, *J. Geophys. Res.*, *104*, 1781–1806.

European Space Agency (1994), Study of the Sun and Moon as radiation calibration targets, technical report, Space Syst. Finland Ltd., Espoo.

Gelinas, R. J., and J. P. Vajk (1981), Diurnal analysis of local variabilities in atmospheric NO$_3$, *J. Geophys. Res.*, *86*, 7369–7377.

Marchand, M., S. Bekki, A. Hauchecorne, and J. Bertaux (2004), Validation of the self-consistency of GOMOS NO$_3$, NO$_2$ and O$_3$ data using chemical data assimilation, *Geophys. Res. Lett.*, *31*, L10107, doi:10.1029/2004GL019631.

McCormick, M. P., et al. (2002), SAGE III algorithm theoretical basis document (ATBD) solar and lunar algorithm, *LaRC 475-00-108*, version 2.1, NASA Langley Res. Cent., Hampton, Va.

Meyer, J., A. C. Schlesier, A. Rozanov, H. Bovensmann, and J. P. Burrows (2004), Towards O$_3$ and NO$_2$ vertical profile retrieval from SCIAMA-CHY solar occultation measurements: First results, *Adv. Space Res.*, *34*, 744–748.

Meyer, J., A. Bracher, A. Rozanov, A. C. Schlesier, H. Bovensmann, and J. P. Burrows (2005), Solar occultation with SCIAMACHY: Algorithm description and first validation, *Atmos. Chem. Phys.*, *5*, 1589–1604.

NASA (1976), U.S. Standard Atmosphere supplements, technical report, U.S. Govt. Print. Off., Washington, D. C.

Naudet, J. P., D. Huguenin, P. Rigaud, and D. Cariolle (1981), Stratospheric observations of NO$_3$ and its experimental and theoretical distribution between 20 and 40 km, *Planet. Space. Sci.*, *29*, 707–712.

Naudet, J. P., P. Rigaud, M. Pirre, and D. Huguenin (1989), Altitude distribution of stratospheric NO$_3$: Observations of NO$_3$ and related species, *J. Geophys. Res.*, *94*, 6374–6382.

Noël, S., H. Bovensmann, M. W. Wuttke, J. P. Burrows, M. Gottwald, E. Krieg, and R. Mager (2000), SCIAMACHY nominal operations and special features, in *4th International Symposium on Environmental Testing for Space Programmes (12–14 June 01 Luik)*, Eur. Space Agency Spec. Publ., SP-467, 1–8.

Norton, R. B., and J. F. Noxon (1986), Dependence of stratospheric NO$_3$ upon latitude and season, *J. Geophys. Res.*, *91*, 5323–5330.

Noxon, J. F., R. B. Norton, and W. R. Henderson (1978), Observation of atmospheric NO$_3$, *Geophys. Res. Lett.*, *5*, 675–678.

Orphal, J., C. E. Fellows, and P.-M. Flaud (2003), The visible absorption spectrum of NO$_3$ measured by high-resolution Fourier transform spectroscopy, *J. Geophys. Res.*, *108*(D3), 4077, doi:10.1029/2002JD002489.

Platt, U., D. Perner, J. Schroeder, C. Kessler, and A. Toenssion (1981), The diurnal variation of NO$_3$, *J. Geophys. Res.*, *86*, 11,965–11,970.

Renard, J.-B., M. Pirre, C. Robert, G. Moreau, D. Huguenin, and J. M. Russel (1996), Nocturnal vertical distribution of stratospheric O$_3$, NO$_2$ and NO$_3$ from balloon measurements, *J. Geophys. Res.*, *101*, 28,793–28,804.

Renard, J.-B., et al. (2001), Measurements and simulation of stratospheric NO$_3$ at mid and high latitudes in the Northern Hemisphere, *J. Geophys. Res.*, *106*, 32,387–32,399.

Rigaud, P., J. P. Naudet, and D. Huguenin (1983), Simultaneous measurements of vertical distributions of stratospheric NO$_3$ and O$_3$ at different periods of the night, *J. Geophys. Res.*, *88*, 1463–1470.

Rodgers, C. D. (1976), Retrieval of atmospheric temperature and composition from remote measurements of thermal radiation, *Rev. Geophys.*, *4*, 609–624.

Rothman, L. S., et al. (1998), The HITRAN molecular spectroscopic database and HAWKS (HITRAN atmospheric workstation), *J. Quant. Spectrosc. Radiat. Transfer*, *60*, 665–710.

Rozanov, A. (2001), Modeling of the radiative transfer through a spherical planetary atmosphere: Application to the atmospheric trace gases retrieval from occultation- and limb-measurements in UV-Vis-NIR, Ph.D. thesis, Univ. Bremen, Bremen, Germany.

Russell, J. M., et al. (1993), The Halogen Occultation Experiment, *J. Geophys. Res.*, *98*, 10,777–10,797.

Sander, S. P., et al. (1997), Chemical kinetics and photochemical data for use in atmospheric modeling, *JPL Publ.*, *12*, 158–160.

Sander, S. P., et al. (2003), Chemical kinetics and photochemical data for use in stratospheric modeling, in *NASA Panel for Data Evaluation, Eval. 14*, JPL Publ., 02-25, 1-119–4-111.

Sanders, R. W., S. Solomon, G. H. Mount, M. W. Bates, and A. L. Schmeltekopf (1987), Visible spectroscopy at McMurdo station, Antarctica: 3. Observation of NO$_3$, *J. Geophys. Res.*, *92*, 8339–8342.

Schlieter, S. (2001), Spurengasmessungen während der Nacht mittels Mondlichtspektroskopie im Vergleich mit Modellrechnungen, Ph.D. thesis, Univ. Bremen, Bremen, Germany.

Sinnhuber, M., J. P. Burrows, M. P. Chipperfield, C. H. Jackman, M. Kallenrode, K. F. Künzi, and M. Quack (2003), A model study of the impact of magnetic field structure on atmospheric composition during solar proton events, *Geophys. Res. Lett.*, *30*(15), 1818, doi:10.1029/2003GL017265.

Smith, J. P., and S. Solomon (1990), Atmospheric NO$_3$: 3. Sunrise disappearance and stratospheric profiles, *J. Geophys. Res.*, *95*, 13,819–13,827.

Solomon, S., H. L. Miller, J. P. Smith, R. W. Sanders, G. H. Mount, A. L. Schmeltekopf, and J. F. Noxon (1989a), Atmospheric NO$_3$: 1. Measurement technique and the annual cycle at 40°S, *J. Geophys. Res.*, *94*, 11,041–11,048.

Solomon, S., R. W. Sanders, G. H. Mount, M. A. Carroll, R. O. Jakoubek, and A. L. Schmeltekopf (1989b), Atmospheric NO$_3$: 2. Observations in polar regions, *J. Geophys. Res.*, *94*, 16,423–16,428.

Solomon, S., J. P. Smith, R. W. Sanders, L. Perliski, H. L. Miller, G. H. Mount, J. G. Keys, and A. L. Schmeltekopf (1993), Visible and near-visible spectroscopy at McMurdo Station, Antarctica: 8. Observation of nighttime NO$_2$ and NO$_3$ from April to October 1991, *J. Geophys. Res.*, *98*, 993–1000.

Wangberg, I., T. Etzkorn, I. Barnes, U. Platt, and K. Becker (1997), Absolute determination of the temperature behavior of the NO$_3$ + NO$_2$ + M = N$_2$O$_5$ + M equilibrium, *J. Phys. Chem. A*, *101*, 9694–9698.

_____

L. K. Amekudzi, H. Bovensmann, J. P. Burrows, L. N. Lamsal, J. Meyer, A. Rozanov, N. V. Sheode, and B.-M. Sinnhuber, Institute of Environmental Physics and Remote Sensing, University of Bremen, Otto-Hahn-Allee 1, D-28359 Bremen, Germany. (leonard@iup.physik.uni-bremen.de)